

**Contract No. and Disclaimer:**

**This manuscript has been authored by Savannah River Nuclear Solutions, LLC under Contract No. DE-AC09-08SR22470 with the U.S. Department of Energy. The United States Government retains and the publisher, by accepting this article for publication, acknowledges that the United States Government retains a non-exclusive, paid-up, irrevocable, worldwide license to publish or reproduce the published form of this work, or allow others to do so, for United States Government purposes.**

# Laser Engineered Net Shaping® for Repair and Hydrogen Compatibility

*LENS technology seems well suited for repair of overbored reclamation-type materials, but additional process development is required for other types of repairs*

BY P. S. KORINKO, T. M. ADAMS, S. H. MALENE, D. GILL, AND J. SMUGERESKY

## ABSTRACT

A method to repair mismachined or damaged components using Laser Engineered Net Shaping® (LENS) technology to apply material was investigated for its feasibility for components exposed to hydrogen. The mechanical properties of LENS bulk materials were also tested for hydrogen compatibility. The LENS process was used to repair simulated and actual mismachined components. These sample components were hydrogen charged and burst tested in the as-received, as-damaged, and as-repaired conditions. The testing showed that there was no apparent additional deficiency associated with hydrogen charging compared to the repair technique. The repair techniques resulted in some components meeting the requirements while others did not. Additional procedure/process development is required prior to recommending production use of LENS.

## Introduction

Manufacturing processes and quality assurance techniques are being continuously improved; however, human error, equipment malfunction, and wear still occur. To address these problems, methods and approaches are continuously being developed to repair these mismachined and worn parts. It is common practice to add virgin metal to worn and mismachined parts using welding, brazing, thermal spraying, plating, etc. (Refs. 1-13). Repair processes are readily available for many components. There is typically substantial inertia to overcome to implement new processes; however, with reduced budgets and compressed time

*P. S. KORINKO, T. M. ADAMS, and S. H. MALENE are with Savannah River National Laboratory, Aiken, S.C. D. GILL is with Sandia National Laboratories, Albuquerque, N.Mex. J. SMUGERESKY is with Sandia National Laboratories, Livermore, Calif.*

scales modern manufacturing facilities must become more agile. This project was conducted to develop an operationally ready capability that is fast, inexpensive, agile, robust, and a repeatable model-based metal component modification and repair system.

The Laser Engineered Net Shaping® (LENS®) technology affords the user two operational modes: 1) complete part/component building or 2) repair/modification of existing parts/components. The focus of this program was on the development and qualification of the LENS technology to repair or modify existing parts and components. This paper provides an overview of the LENS technology and a detailed discussion of the capability of the process to repair mismachined or damaged components. It also demonstrates the hydrogen compatibility of the LENS material in bulk as well as the Savannah River National Laboratory (SRNL) selected repair application.

## Process Overview

The LENS process utilizes a laser and powdered metal to form metal parts from computer solid models. The basic system consists of a laser, a powder feeder, a set of motion-controlled axes, a substrate material, an inert atmosphere, and a closed-loop melt pool control system. A 3-D model of the process is shown in Fig. 1. The laser is focused on a metal substrate creating a small molten pool. The powder feeder feeds powdered metal into a flowing argon stream that is directed into the melt pool by four nozzle tips. The powdered metal melts and then the melt pool

solidifies as the "axis" moves, via stepper motor, the melt pool to a new location. When moved smoothly along a trajectory, a raised deposit of the desired material is applied. The previously programmed computer-aided design (CAD) model controls the development of the part; the model represents the desired additional material as layers and each layer is divided into lines. The repair or component fabrication proceeds by depositing material line by line and layer by layer.

Figure 1 also shows several of the most important process parameters that can be varied to change the properties of the part. The laser power has to be balanced so that it is sufficient to melt the powder but not so high as to ablate the material. In many instances, this is controlled by a closed-loop melt pool controller that applies a proportional-integral-differential (PID) controlled feedback loop to maintain a constant area of the melt pool, based on the reflectance of the image, above some chosen intensity value. The powder flow rate is controlled as well. More powder builds taller parts, but excessive powder flow can cool the melt pool to such a point that the metal powder is not fused, resulting in inclusions and pores in the finished part. The layer thickness determines how much of the previous layer is remelted in the current layer. Too large a layer thickness will also cause the laser focus to advance too quickly for the material, ending in a part that does not meet geometric requirements. The hatch width determines the amount of mixing between lines deposited within the same layer. And the axis feed rate determines how fast the melt pool cools in addition to affecting the height of the build by increasing or reducing the amount of time that the melt pool is available to receive powder at a certain position.

Sandia National Laboratory's (SNL) LENS machine is shown in Fig. 2. The system is composed of five major subsystems: a) a laser subsystem of sufficient size to melt metal and the wavelength determines the laser's compatibility with specific materials (SNL's system utilizes a 1200-W, continuous wave, Nd-YAG laser); b) a closed-loop melt pool control system that

## KEYWORDS

Laser Engineered Net Shaping (LENS)  
Reclamation Welding  
Hydrogen  
Baseline

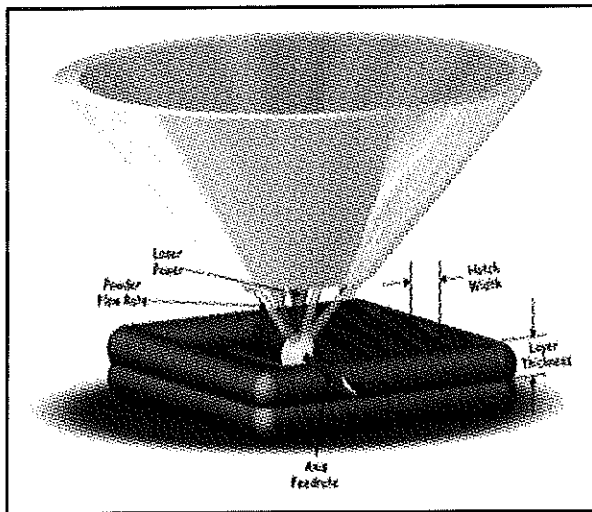


Fig. 1 — The LENS process showing important process parameters.

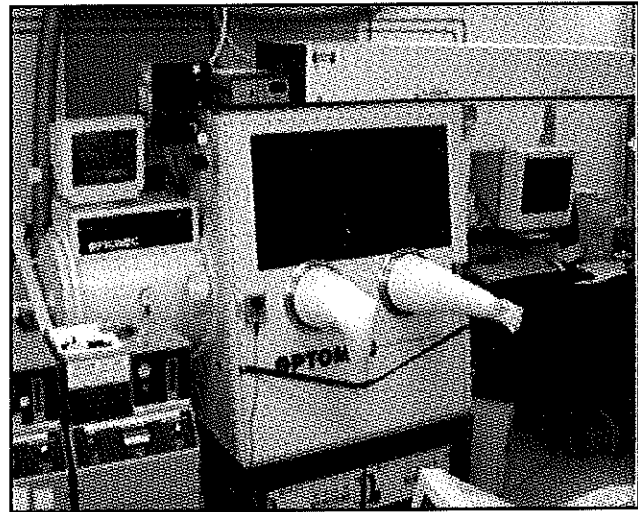


Fig. 2 — Sandia National Laboratory's LENS processing machine, which is composed of a laser, closed-loop melt pool control system, motion control system, powder delivery system, and environmental chamber.

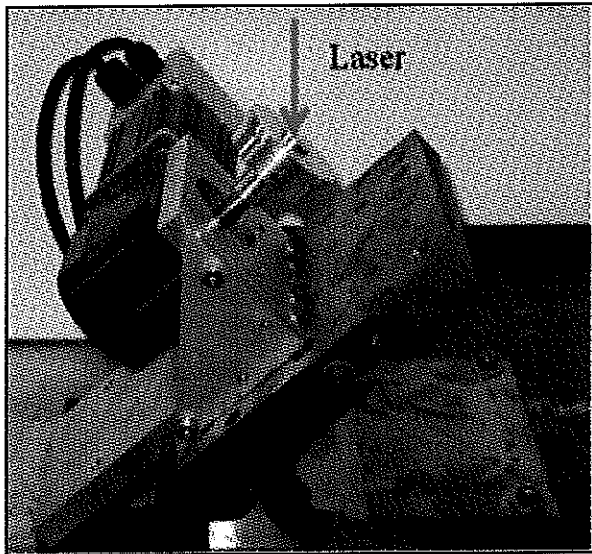


Fig. 3 — The reclamation weld bases were repaired using the 4th axis mounted in the LENS machine at 45 deg to horizontal.

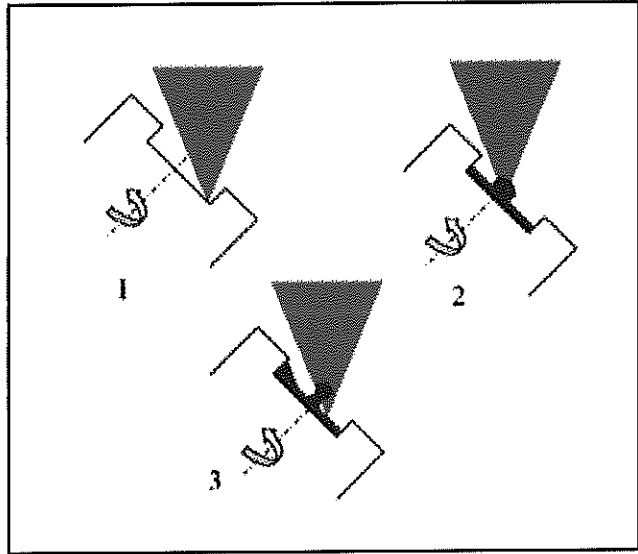


Fig. 4 — The repair proceeded from the outside to the center of the bore with the axis greatly increasing in rotational speed for each subsequent ring.

works closely with the laser to create consistent, repeatable process conditions; c) a motion control system that uses coordinated movements of a set of axes (the motion must be controlled to create the component in the desired geometry); d) a powder delivery system that typically consists of a stream of pressurized process gas, one or more powder feeders to meter powder into the gas stream, and a powder distribution system; and e) a purified environment (typically argon with <5 ppm oxygen) to ensure the material deposited is as similar as possible to the composition of the metal powder used in the process.

The LENS® process (Refs. 21–25) has been demonstrated for a variety of materials and part configurations. LENS® technology has successfully processed: 1) stain-

less steels (Types 316, 304L, and 309S); 2) nickel alloys (Inconel® 718, 625, and 690); 3) tool steels (H-13, NU-Die EZ, MM-10, and CPM-10); 4) titanium alloy Ti-6Al-4V;

5) aluminum alloys; 6) gamma titanium-aluminide; 7) tungsten; and 8) metal matrix composites (WC in Co). In this project, we were concerned only with the applicability

Table 1 — The LENS® Process Parameters Used for Reclamation Base Repairs as Compared to Process Development Parameters Determined for Large Drill Blocks

	Process Development Block	Reclamation Base
Powder Flowrate (gal/min)	23 (400 rpm)	23
Laser Power (W)	355–480 W (26–28 A) - 575 W 1st layer	535 W (29 A)
Filter %	80%	70%
WP Intensity	400/150	—
Fill Area (pix)	750/650	—
Border Area (pix)	750/650	—
Axis Feedrate (in./min)	22/20	22+ (faster near center)
Material	304L Drill Blocks	Virgin 304L

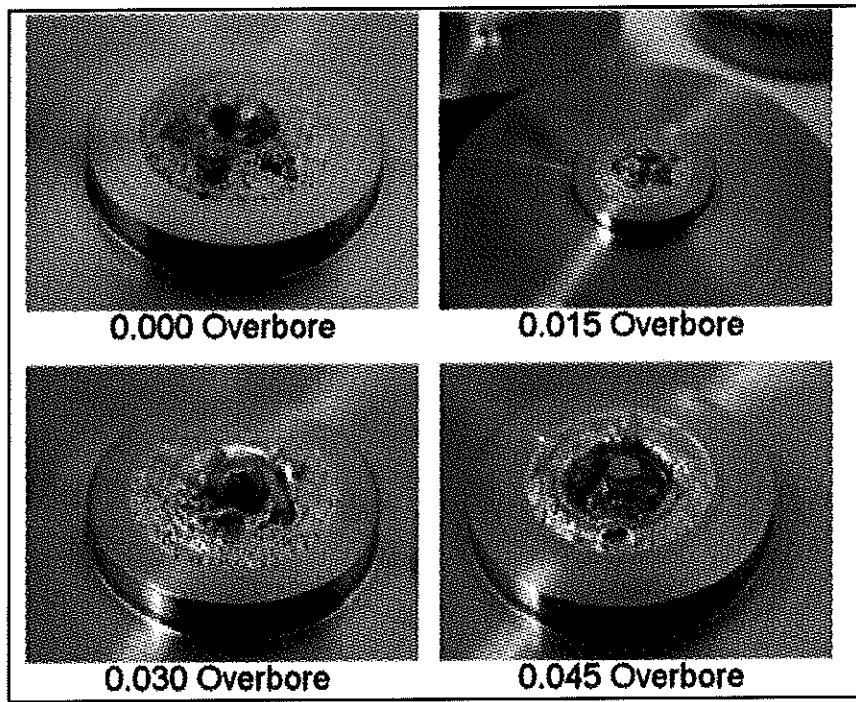


Fig. 5 — The repaired bores had excellent adhesion to the walls and bottom of the bore, but the material was not high quality at the center.

of the process with 304L stainless steel. With this understanding of the process, one can proceed with the implementation of LENS as a repair technology for the SRNL-specific components.

#### Experimental

Two components were considered for repair development. The first was a hydrogen gas vessel that may be prepared using a solid-state resistance forge weld of a "reclamation" stem into a machined bore. During preparation, it is possible to bore the hole to wrong depth or wrong diameter or to bore the hole eccentrically. These machining errors can be simulated simply by overboring the hole so reclamation test bases were fabricated with bores that were 0.015, 0.030, and 0.045 in. (0.38, 0.76, and 1.14 mm) larger than typically specified. In addition, the largest hole was increased in depth by 0.015 in. (0.38 mm).

The other simulated repair that was of interest was surface anomalies and scratches. The typical depth of the scratches of concern is on the order of a few ten thousandths of an inch. Due to the difficulty in defining scratch depths of this nature, it was decided to create machined defects that were 0.10, 0.020, and 0.030 in. deep (0.25, 0.51, and 0.76 mm) on gas bottles with a 0.060-in. (1.52-mm) wall.

#### Mechanical Property Sample

A monolithic block of 304L stainless steel was prepared using the LENS process.

This material was deposited using typical 304L stainless steel application processes. The conditions are presented in Table 1. These conditions are typical of the parameters for Type 304L SS and are based on the extensive knowledge and experience of SNL. This prepared material was used for microstructure and preliminary mechanical property testing.

#### LENS Repair of Overbored Reclamation Weld Bases

Sample reclamation test weld bases with overbored stem holes were also prepared for LENS® repair. In the actual reclamation process, an old welded stem is removed by milling, the hole is rebored to achieve proper position and size, and a new stem is solid-state resistance welded (RW) into place. The provided bases had sample defect holes that had been overbored such that diameters were too large by 0.015, 0.030, and 0.045 in. (0.38, 0.76, and 1.14 mm). In addition to being overbored, the largest diameter was also bored 0.015 in. (0.38 mm) too deep. The challenge for the process was to add dense, well-bonded material such that the hole could be rebored to the correct diameter, a new stem welded in place, and the sample hydroburst tested. Several of the welds were then sectioned to inspect the interfaces between LENS, base, weld, and stem materials.

The bore was filled utilizing a 4th axis unit mounted in the LENS machine with the axis of rotation at an angle of 45 deg

from horizontal, as shown in Fig. 3. This approach was used to allow the laser to deposit material on the bottom of the bore as well as the walls. Concentric rings of material with decreasing radii were deposited on the bottom of the bore from the outside to the center. The laser then incremented up one layer and deposited the next layer from the outside to the center again. In this way, the bore was filled. In the initial efforts, the rotational speed of the weld base on the 4th axis was increased as the radius of deposit was decreased such that the apparent feed rate remained constant regardless of radius size. The method presented several challenges, however. As seen in Fig. 4, as the laser approached the center of the bore, the heat built up and caused excess powder to be entrained in the melt pool, thus creating a bump. By the second pass, the bump became tall enough to grow into the beam even when the laser was depositing at the outer edge. This caused the beam to be obscured at the outer edge and caused the bump to grow at a very high rate all the time. To address this issue, the rotational speed of the axis was increased near the center to considerably higher speeds than used previously. In addition, the very center of the part was not filled on the first several passes. This allowed high-quality material to be deposited on the walls of the part without obscuring the center. It did mean that the center material did not adequately fuse with the layer below it. This attribute was not important since the center of the hole is sacrificial material and would be removed as part of the RW preparation of the test bases. In fact, the center material was just provided to allow the hole to be drilled, if desired, rather than helically interpolated with a mill, which is a more time-consuming process.

Figure 5 shows the as-repaired condition of the deposit from a macro standpoint. It is important to note that differences in the appearance and the apparent density and crowning of the fill are not due to the diameter of the oversize bore, but are instead due to process improvements made throughout the repair of these components. The 0.045-in. (1.14-mm) overbore bases were done first and have the least desirable center bump. The 0.030-in. (0.76-mm) overbore bases had the improvement of higher rotational speed near the center of the deposit, and the 0.000- and 0.015-in. (0.38-mm) overbore bases had further improvements in that the center of the bore did not have additive material for the first layers. The zero overbore sample has a slightly improved definition of where the final radius should be for each layer. A difficulty for the process development was that the LENS

material deposition team only had two process setup pieces which was insufficient for optimizing the deposition approach. As shown by Fig. 5, considerable improvement in the appearance of the samples is evident from the 0.045-in. (1.14-mm) overbore to the 0.015-in. (0.38-mm) overbore, or from the first to the seventh component (the first of the 0.015-in. overbore repairs). Additionally, as the amount of overbore changed, the diameters of the deposited rings changed, which added another variable to the process development challenges.

In addition to filling the weld base bores, the bases had surface flaws to be repaired. These flaws were developed to be typical of shipping, usage, and handling scratches as might be found on any part that had been through a number of machining processes. The repaired scratches are shown in Fig. 6 with the radial deposit lines showing the location of the scratches. The challenge of repairing these flaws is that the flaws were truly random (created with a hand awl) so process planning was a bit challenging. However, by "blipping" the laser on and off, the end points of straight lines were determined that would cover the flaws.

The process parameters used for the bores are given in Table 1 where they are compared to process parameters determined for large block samples, used for tensile testing, of the same 304L material. In contrast to the description presented earlier, the reclamation weld base repairs were all performed without the closed-loop melt pool controller since the controller was getting false signals from reflections off the walls of the bore.

#### LENS Repair of Sample Bottle Surface Flaws

The second set of components provided for LENS repair was gouged sample gas bottles. These items represented bottles that are rejected by the customer if there is any visible surface flaw on them, which is typically less than 0.001 in. (0.025 mm) deep. These test sample gouges were milled into each bottle. The gouges were 0.125 in. (2.5 mm) wide and either 0.010 in. (0.25 mm) or 0.020 in. (0.51 mm) deep, and were made by a parallel-sided end mill as shown in Fig. 7. The bottles were positioned in the LENS machine in a V block and toe clamped as shown in Fig. 8. The bottle was positioned against a pin at the end of the V block for positioning and a V-block clamp was used to roll the bottle until the gouge was perpendicular to the laser axis and centered. The toe clamps were then lightly tightened to hold the bottle. The laser, set at low power, traced the edges of the gouge to check alignment. The LENS repair then occurred with the laser depositing two or three layers [for 0.010- and 0.020-in.- (0.25-

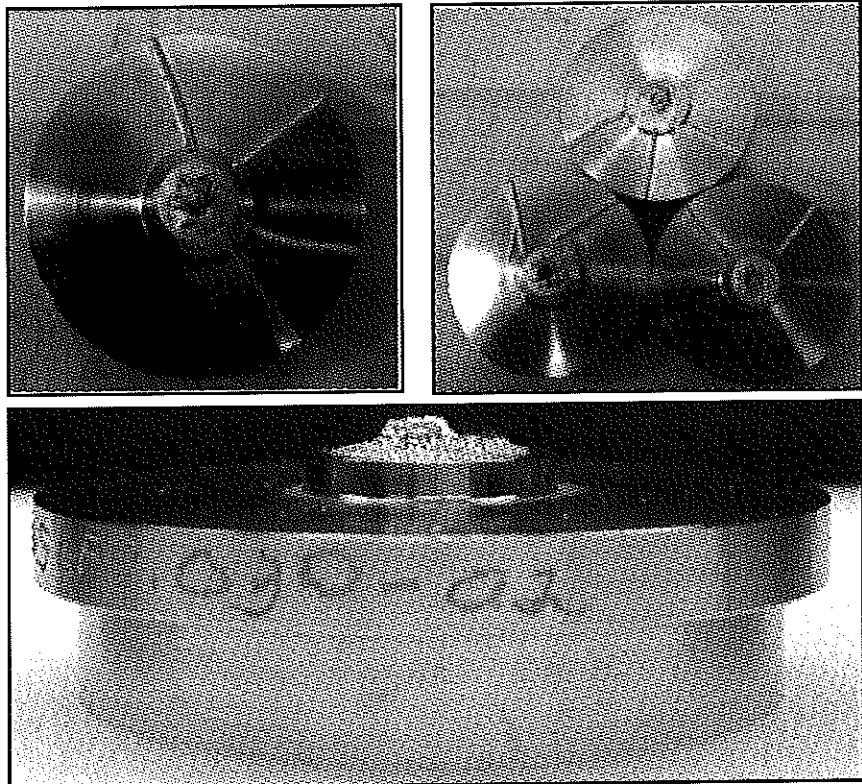


Fig. 6 — Bore and radial repaired scratches on the surface of the weld bases.

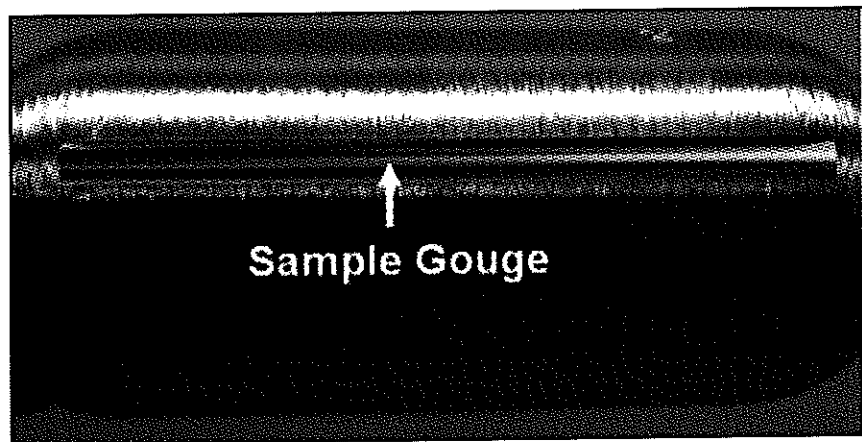


Fig. 7 — Sample gouge in sample gas bottle. Gouges were 0.125 in. wide and either 0.010 or 0.020 in. deep.

and 0.51-mm) deep gouges, respectively], as shown in Fig. 9. Due to the limited number of samples prepared and programmatic restraints, neither postrepair metallography nor radiographic examination were conducted. The process parameters for the bottle repair are given in Table 2 for comparison with the process parameters determined for the deposition of the monolithic blocks.

#### Hydrogen Compatibility Testing

It is widely known that austenitic stainless steels perform better than other types of stainless steel in hydrogen environ-

ments. A critical aspect for using repaired components in a hydrogen environment is understanding the interactions between hydrogen and various materials used in process, handling, and storage systems. For this program, 304L was selected as the material of interest for evaluation since it is a major component of various components exposed to hydrogen. To determine the effect of hydrogen on LENS-repaired components, two aspects were studied. The initial effort focused on the evaluation for hydrogen compatibility of baseline materials for LENS processed 304L. Following this initial material properties evaluation, the program considered the

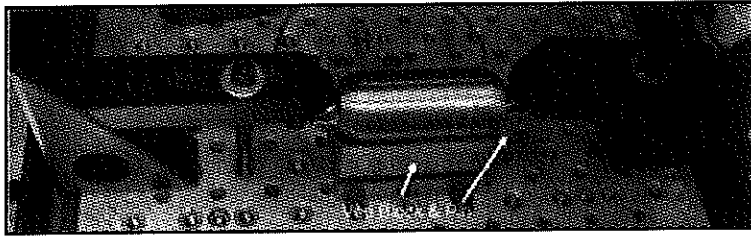


Fig. 8 — Mounting fixture in LENS machine holding bottle for repair.

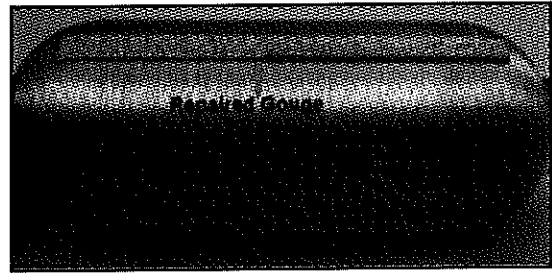


Fig. 9 — Repaired gouge in sample gas bottle.

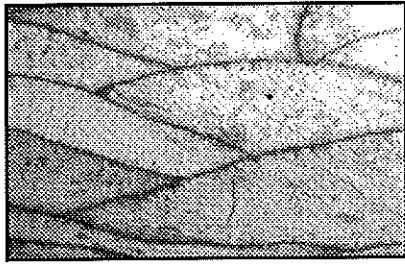


Fig. 10 — Representative microstructure of as-processed 304L LENS materials [polished and electrolytically etched (10% oxalic acid)].

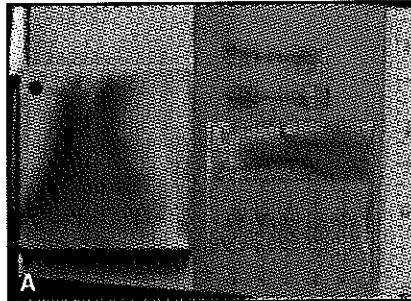


Fig. 11 — A — 8-cm block of 304L LENS-processed material and EDM harvested tensile dogbones; B — tensile testing 304L LENS materials.

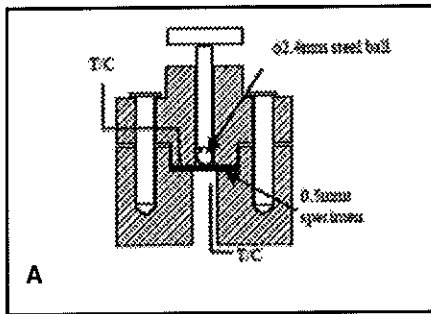


Fig. 12 — A — Schematic of small sample punch test; B — SRNL punch test apparatus.

repair or modification of representative components using LENS and the subsequent performance of these parts and components following repair or modification in the baseline and hydrogen-charged condition. As was discussed previously, the components selected for repair by SRNL were gas bottle reclamation weld

bores and gas bottle surface defects.

#### Microstructure and Mechanical Properties of LENS® Processed Material

*Microstructure Characterization of 304L LENS Materials.* A sample from the 8-cm block of 304L LENS materials fabricated

by SNL was sectioned, mounted, polished, and examined using light optical microscopy. The multilayered structure displayed in Fig. 10 is characteristic of LENS-deposited materials and depicts the nature of the multipass deposition technology with very fine grains and interpass and interlayer interfaces. Unfortunately, higher magnification images were not taken so the solidification morphology and primary solidification mode cannot be discerned.

*Mechanical Behavior of LENS-Processed Material in Hydrogen.* A challenge to the successful qualification and acceptance of LENS-processed materials for service in hydrogen isotope applications is the ability to demonstrate that the mechanical properties are at least comparable to conventional materials. As such, the focus of this task was to evaluate the tensile properties, including yield strength, ultimate tensile strength, and elongation to failure, of LENS materials in both the uncharged and hydrogen-charged conditions. No attempt will be made to compare LENS material properties to the production forged, pedigreed gas transfer bottle materials. Sub-miniature tensile dogbone samples were machined from an 8-cm<sup>3</sup> (3.15-in.) block of 304L LENS materials prepared by SNL — Fig. 11A. The samples were fabricated using electric discharge machining (EDM) at SRNL. Comparison samples were machined from 0.020-in.- (0.51-mm-) thick 304L commercial sheet stock material. The tensile dogbone samples had a 0.5-in. (12-mm) gauge length and an overall sample length of 1.25 in. (31.7 mm). The tests were conducted on

Table 2 — LENS® Process Parameters for Sample Gas Bottle Surface Flaws Compared to Parameters for LENS® Deposit of Large 304L Blocks

	Process Development	Surface Flaw
Powder Flow Rate (gal/min)	23 (400 rpm)	37
Laser Power (W)	350–400 W (26–28 A) – 575 W 1st layer	—
Filter %	80%	70%
WP Intensity	400/150	300
Fill Area (pix)	750/650	750
Border Area (pix)	750/650	750
Axis Feedrate (in./min)	22/20	22
Material	304L Drill Blocks	Virgin 304L

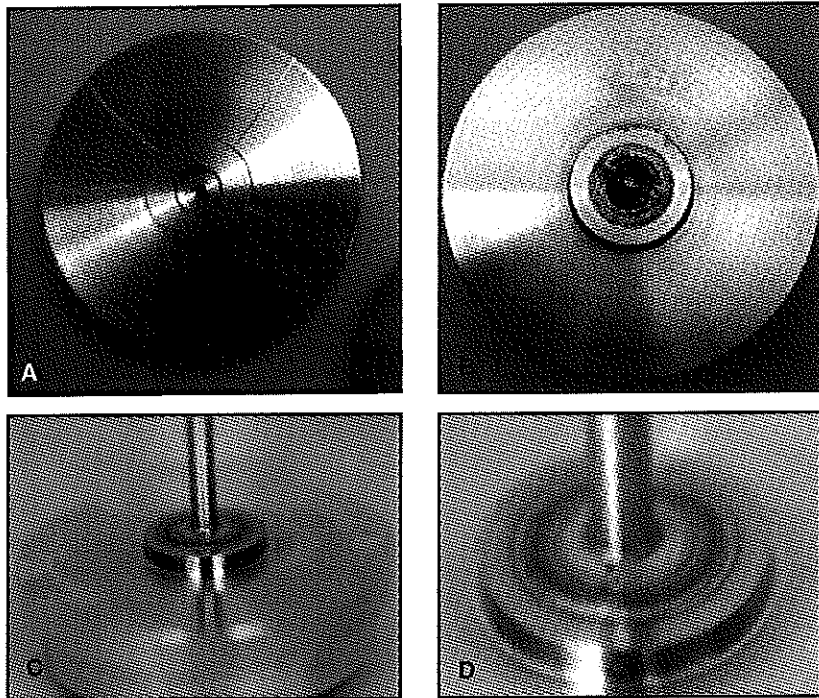


Fig. 13 — LF-7 test base in the following conditions: A — As machined; B — as LENS repaired; C and D — as welded.

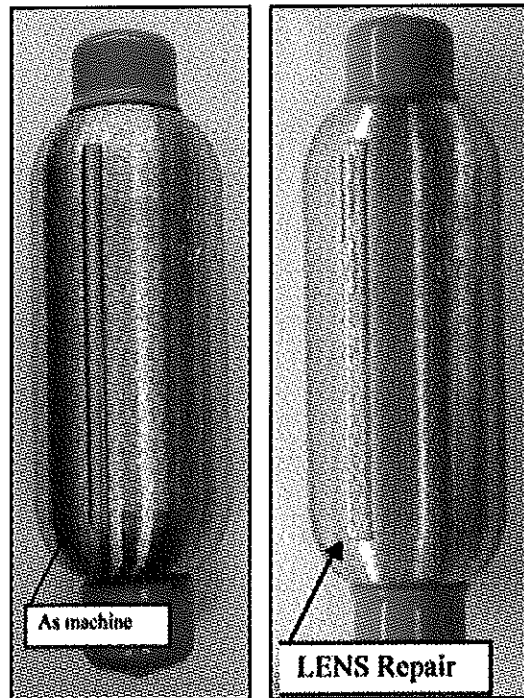


Fig. 14 — As-machined (notched), as-LENS-repaired, and as-final-machined gas sample bottles.

samples charged for 5 days at 2500 lb/in.<sup>2</sup> (17.2 MPa) H<sub>2</sub> at 325°C, which should yield 4.4 cc H<sub>2</sub> per cc metal. Testing was performed at room temperature in air using a screw-driven testing machine with pneumatic grips and a cross-head speed of 0.002 in./min (0.051 mm/min). The load was measured by the load cell on the machine, and the gauge length displacement was measured with a clip gauge attached directly to the sample — Fig. 11B.

In addition to this tensile mechanical testing, some small sample punch tests were performed to compare the fracture toughness behavior of hydrogen-charged with uncharged LENS-processed 304L material. This technique is amenable to small sample sizes and the experimental setup is rather simple. The arrangement of the technique is shown in Fig. 12A. Tests are conducted on samples approximately 0.118 in. (3 mm) in diameter and 0.008–0.012 in. (0.5–0.75 mm) in thickness. A load is placed on the disk sample via the tensile load frame cross-head pushing on the punch rod of the test apparatus. Typical cross-head speeds of 0.004–0.008 in./min (0.1–0.2 mm/min) are employed. As a relative measure of fracture toughness, several empirical relations have been developed in the literature (Refs. 16–18). Using the original sample thickness and the deflection at sample failure, the biaxial fracture strain is calculated. Using this calculated biaxial fracture strain and an empirically determined relationship between biaxial fracture strain and measured

ductile fracture toughness, J<sub>IC</sub> values can be estimated. Punch test samples were also machined from an 8-cm<sup>3</sup> block of 304L LENS materials prepared by SNL — Fig. 11A. The samples were fabricated using EDM similarly to the tensile samples discussed above. The punch samples were approximately 0.118 in. (3 mm) in diameter and 0.010 in. (0.025 cm) in thickness. The tests were conducted on samples charged for 5 days at 2500 lb/in.<sup>2</sup> (17.2 MPa) H<sub>2</sub> at 325°C which should yield 4.4cc H<sub>2</sub> per cc of metal. Testing was performed at room temperature in air using a screw-driven testing machine with a 1-mm-diameter tungsten carbide ball at a cross-head speed of 0.008 in./min (0.203 mm/min) while recording load and cross-head displacement via a gauge attached to the compression platen.

#### Sample Preparation

Reclamation welds were made using the nominal weld parameters for common production-type test bases fabricated from Type 304L stainless steel, i.e., 2250-lb (5.56-kN) loading force, 11,400-A welding current, and 25 weld cycles based on a 60-Hz weld process current. All of the welds were performed in a manner consistent with the production weld parameter range. Typical reclamation test bases in the as-machined, as-repaired, and as-welded conditions are shown in Fig. 13. There is a small amount of heat banding and some material extrusion around the

weld; these features are typical of normal production reclamation welds.

Commercial gas sample bottles, formed by hot spinning and subsequent grinding, were also tested to determine the effect of deep scratches on the burst test characteristics. Sample bottles were prepared for LENS repair by milling a 1/8-in.-wide notch to a depth of either 0.010 or 0.020 in. deep and LENS repairing the notch. This defect represents a worst-case scenario for small scratches on a reservoir that would result in rejection of the reservoir. The vessels were turned to remove the excess LENS material. The surface condition of the gas sample bottles in the as-milled, as-welded, and as-final-machined conditions is shown in Fig. 14. The vessels were machined to the extent needed to remove the weld reinforcement; no vessel wall material was removed. Since only the minimum material was removed, the entire LENS repair did not clean up. The residual stresses due to the repair process are the most likely cause for the remaining depression in the vessel.

#### Hydrogen Charging

An autoclave engineer's 1-gal vessel was used to charge the samples. The vessel is rated at 3500 lb/in.<sup>2</sup> (24.1 MPa) [at 650at°F (343°C)] and is made from stainless steel. The vessel is heated by three heater bands that were powered using a PID-controlled power supply. The sam-

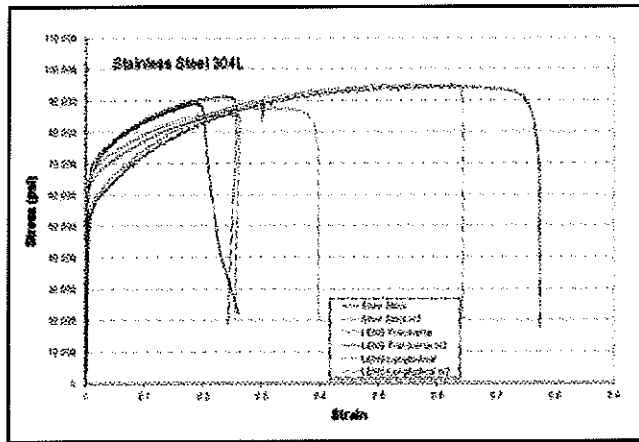


Fig. 15 — Tensile testing curves for 304L sheet stock and LENS materials in the hydrogen-charged and baseline conditions.

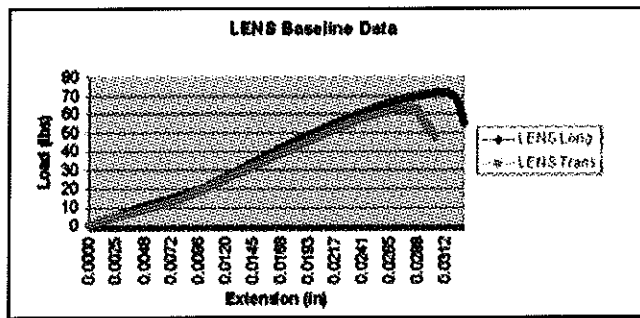


Fig. 16 — Small sample punch testing curves for Type 304L LENS materials in the following conditions: A — Baseline; B — hydrogen charged.

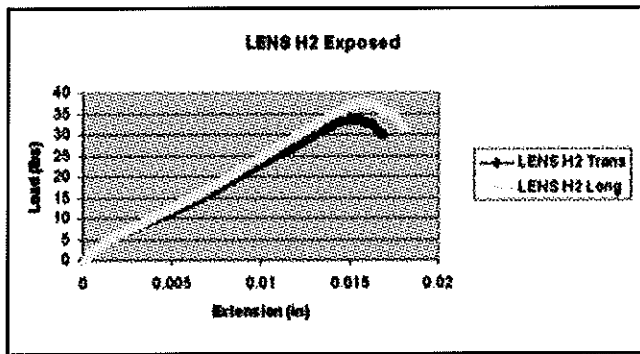


Fig. 17 — Hydroburst pressures for baseline, lens repaired and hydrogen charged fill stems show that no adverse effects are indicated.

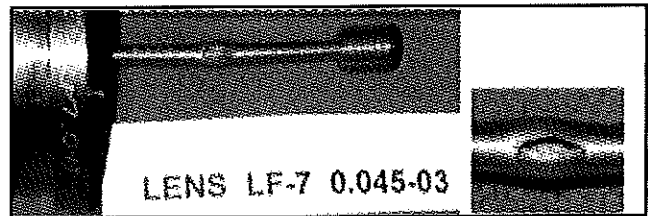


Fig. 18 — Burst tested 0.045-in. overbore and LENS-repaired and reclamation-welded sample.

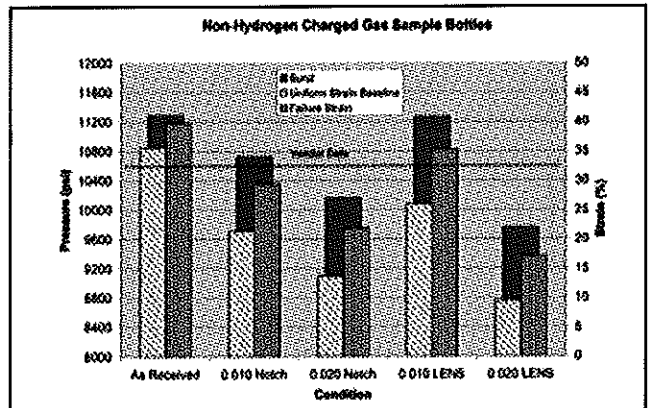


Fig. 19 — Effect of notches and LENS repair on burst properties of gas sample bottles.

ples were placed in the vessel with the gas samples on the bottom and the reclamation welded samples on top. The vessel was approximately 60% filled with hardware. The top cover was installed and

argon was used to purge air from the system and internal surfaces of the test articles. After about 20 min, hydrogen at a pressure of 1500 lb/in.<sup>2</sup> (10.3 MPa) was introduced. The vessel was then heated

to 617°F (325°C), the pressure increased to approximately 2500 lb/in.<sup>2</sup> (17.2 MPa) and held for four days. These conditions are predicted to result in 4.4 cc H<sub>2</sub> per cc metal. These test conditions were deemed adequate to achieve greater than 95% hydrogen saturation based on SRNL Diff94 permeation calculations; this program uses a finite difference with published data for solubility and diffusivity to calculate hydrogen concentration profiles. At least one sample of each manufacturing defect and LENS repair condition was tested without hydrogen charging so the effect of hydrogen on the sample could be ascertained. There was some hydrogen pressure decay that is likely due to some leakage as well as hy-

Table 3 — Estimated Decrease in Fracture Toughness for 304L LENS® Materials Exposed to Hydrogen

Material and Condition	$\epsilon_{qf}$	Estimated $J_{IC}$ (kJ/m <sup>2</sup> )
LENS® 304L Longitudinal — Air	1.250	300
LENS® 304L Transverse — Air	1.112	261
LENS® 304L Longitudinal — Hydrogen	0.630	126
LENS® 304L Transverse — Hydrogen	0.564	108

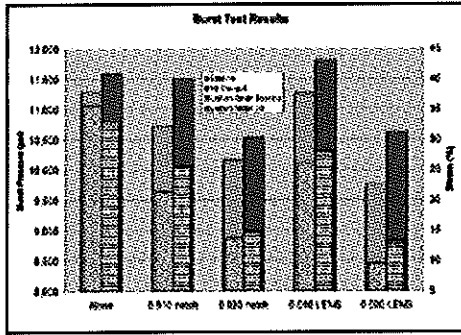


Fig. 20 — Effect of hydrogen on baseline and LENS-repaired samples.

drogen uptake by the samples, since the vessel did not have an active pressurization control loop, no adjustments for the loss of pressure were made. The samples were cooled under hydrogen pressure, removed from the vessel and tested.

### Results and Discussion

Typical results from the tensile testing and small sample punch testing of 304L LENS samples are shown in Figs. 15 and 16. The tensile curves in Fig. 15 show that for both the longitudinal and transverse sample directions (longitudinal and transverse to the build direction of the 8 cm<sup>3</sup> block), there is little difference in the yield strength (YS) and ultimate tensile strength (UTS) comparing identically oriented samples exposed to hydrogen to those not exposed. The largest difference between the unexposed and exposed samples occurs with respect to the percent elongation to failure (%EL). The %EL in both orientations decreased following exposure of the materials to hydrogen. This indicates the reduced ductility from hydrogen embrittlement, which would manifest itself potentially in reduced fracture toughness. Examination of literature data for 304L in both the unexposed and hydrogen-exposed conditions shows a similar trend — little change, to some strengthening — in the tensile properties of YS and UTS with greater change in the %EL upon exposure to hydrogen (Ref. 26). Further analysis of this literature fracture data for samples that exhibited reduced %EL upon exposure to hydrogen have shown a reduction in the ductile fracture toughness on the order of 25–40%.

Analysis of the small sample punch test data in Fig. 16 to estimate the reduction in fracture toughness of the LENS process 304L material upon exposure to hydrogen has been performed. Calculation of the biaxial fracture strain  $\epsilon_{qf}$  using Equation 1,

$$\epsilon_{qf} = 0.15 (\delta/t_0) \quad (1)$$

in both the longitudinal and transverse direction, shows that the estimated strain at

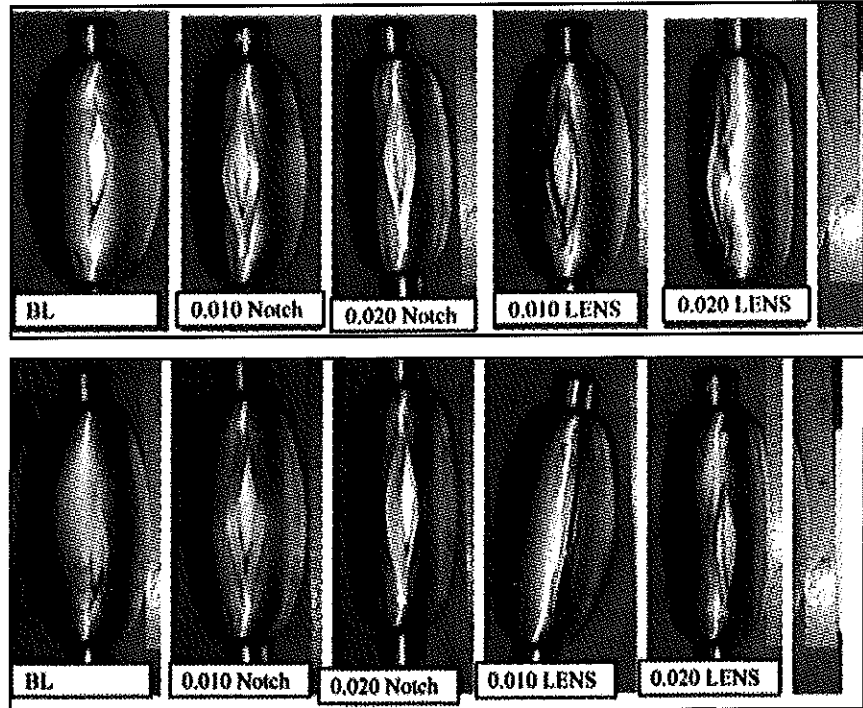


Fig. 21 — Burst test gas sample bottles: A — As received; B — hydrogen charged.

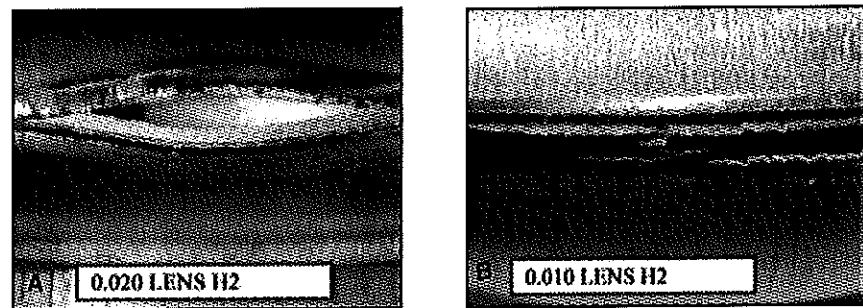


Fig. 22 — Expanded view of hydrogen-charged and tested samples: A — Repaired over a 0.02-in. notch; B — repaired over 0.010-in. notch that failed in the body, not the repair.

fracture for both directions upon exposure to hydrogen decreases on the order of 50%. Estimation of the ductile fracture toughness values using the  $\epsilon_{qf}$  and the empirical relationship, Equation 2,

$$J_{IC} \text{ (kJ/m}^2\text{)} = 280 \epsilon_{qf} - 50 \quad (2)$$

is given in Table 3. Examination of the trend for the estimated ductile fracture toughness values in Table 3 shows that hy-

Table 4 — Preparation and Charging Conditions and Test Results for the Reclamation Test Samples and Hydro Burst Results

Sample	Charged	Burst Pressure (lb/in. <sup>2</sup> )
LF-7 0.000 3	N	56,172
LF-7 0.000 2	Y	56,819
LF-7 0.000 1	Y	57,668
LF-7 0.015 3	N	61,243
LF-7 0.015 2	Y	63,180
LF-7 0.015 1	Y	59,864
LF-7 0.030 3	N	59,471
LF-7 0.030 1	Y	62,289
LF-7 0.030 2	Y	62,113
LF-7 0.045 1	N	61,752
LF-7 0.045 2	Y	63,406
LF-7 0.045 3	Y	62,490

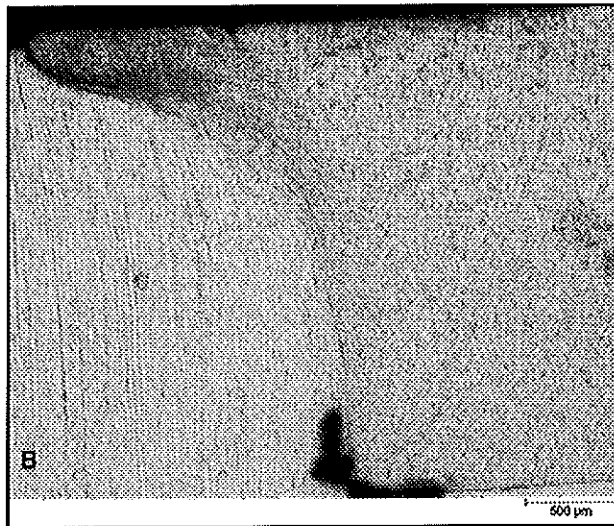
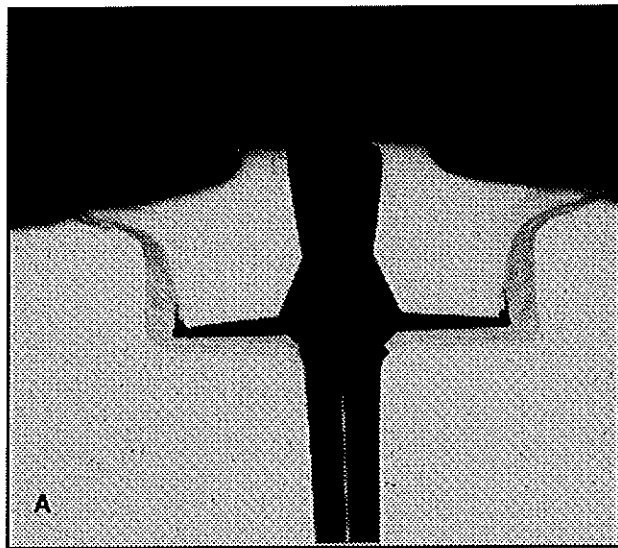


Fig. 23 — A — Metallographic cross section of a burst tested, LENS-repaired 0.045-in. overbore reclamation weld; B — typical Type 304 SS reclamation weld in the as-welded condition (note parallel nature of foot base and reclamation base).



Fig. 24 — Typical area of a LENS-repaired sample that had a 0.020-in.-deep notch machined into it.

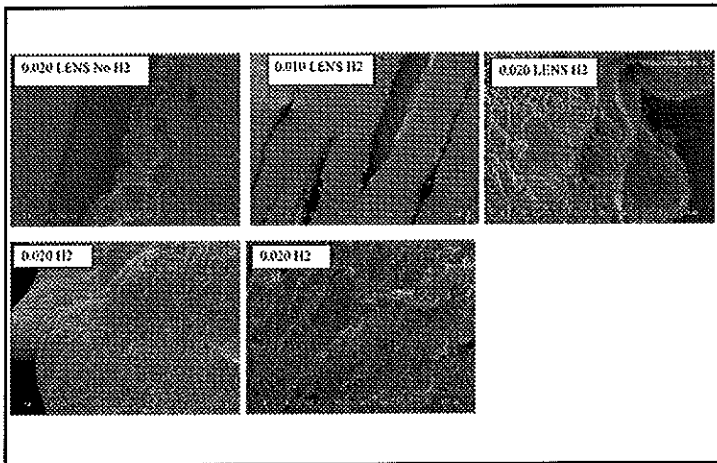


Fig. 25 — Burst test sample fractography.

drogen exposure decreases the fracture toughness and that the transverse orientation appears to be more susceptible.

#### Burst Testing Reclamation Test Bases

The reclamation test samples and bottles were burst tested using hydroburst testing equipment. The samples were connected to the high-pressure fittings and pressurized to failure in about 1 min. The burst tests were videotaped so the burst location could be observed.

All of the reclamation test welds failed in the fill stem tube wall at a pressure of approximately 58 to 62 ksi, which is consistent with the expected material properties of these stems. A graph of the data is shown in Fig. 17 and a photograph of a typical burst tested reclamation test stem is shown in Fig. 18. It can be seen that the tube split and formed a fingernail-type breach. The test results for the reclamation test base samples

are listed in Table 4. Failure in the tube wall is expected since the strength of the weld and the length of the effective bond would have to be less than half the wall thickness if the stem were to fail in any other manner, based on a comparison to the thin wall pressure vessel calculations (Ref. 31) where

$$\sigma_{\text{hoop}} = \text{pressure} * \text{radius}/\text{thickness} \quad (3)$$

and

$$\sigma_{\text{axial}} = \text{pressure} * \text{radius}/(2 * \text{thickness}) \quad (4)$$

Thus, it is apparent that the axial stress, i.e., the location of the LENS material that is bonded to the test base, will be 1/2 that of the hoop stress.

#### Burst Test Gas Sampling Bottles

The sample bottles were sealed on one end with a threaded plug and fitted with a high-pressure fitting on the other end for pressurization. The vessels were filled

with water using a hypodermic needle. The bottles were then attached to the system piping and were pressurized to failure in approximately 1 min. The vessels all exhibited a longitudinal tear that apparently initiated near the center of the vessel, which would be at the location of the highest strain. The data for the as-received sample bottle are comparable to the vendor certification data for these vessels (Table 5). The as-notched samples in the uncharged condition exhibited a reduction in both burst pressure and failure ductility. LENS repair for a 0.010-in.-deep notch is able to restore the burst pressure; however, the uniform strain (ductility) is not fully restored — Fig. 19.

The hydrogen-charged samples exhibit interesting results. The baseline data shown in Fig. 19 are repeated in Fig. 20 along with the hydrogen sample data. The hydrogen-charged samples show some strengthening due to hydrogen charging.

This phenomenon has been seen in previous tensile test work (Ref. 26). The hydrogen data plotted in Fig. 20 are the average of the two points for each condition indicated in Table 5. As was the case for the baseline samples, the presence of notches reduced the burst pressure for hydrogen-charged samples, although the fractional reduction in burst pressure was less for the hydrogen-charged samples than the baseline. The burst ductility is lower for the hydrogen-charged samples with notches.

The sample with the 0.010-in. (0.25-mm) notch that was LENS repaired demonstrated a slight increase in strength over the baseline condition for hydrogen charging and essentially no loss from the baseline value. Both the 0.020 in. (0.51 mm) notched and 0.020 in. (0.51 mm) notch and LENS-repaired sample exhibit burst pressures and uniform strains of 23 and 20%, respectively, compared to 40% for the baseline sample.

The appearance of the burst tested gas sample bottles exhibited the expected failure with the bottle opening up axially; in addition, all of the samples with notches failed in the notch. There was one exception for the LENS-repaired samples: Sample 0.010 LENS-repaired 1, which failed in the vessel body away from the LENS repair, suggesting an excellent repair and no adverse impact on strength. Macro photographs of the burst-tested vessels are presented in Fig. 21. The baseline samples are presented in Fig. 21A and the hydrogen-charged samples are presented in Fig. 21B. The change in sample diameter growth, i.e., direct indication of strain, is apparently lower as the extent of the defect increases.

The fracture surfaces of the LENS repaired surfaces were also examined. The LENS material appears to have cracked axially and some of the samples exhibit a possible delamination. This failure mode may be indicative of the deposition method and deposition direction. The cracking and onset of delamination of sample 0.010 LENS H<sub>2</sub> that did not fail in the LENS repair area is shown in Fig. 22.

The LENS repairs for the sample gas bottles were generally successful with the repaired gouges having an acceptable appearance as shown in Fig. 14. Upon hydrogen charging and burst testing, the bottles all passed the required pressure before bursting, but the bottles did burst along one edge of the gouge. Further analysis and sectioning showed that the LENS material did not quite fill the bottom corner of the gouge in some cases. This bottom corner of the gouge acted as a stress riser causing failure to initiate at the site. To achieve better results in the future, it is suggested that a ball end mill or angled mill be used to make the bot-

Table 5 — Hydrogen-Charged Samples Data (Shown graphically in Fig. 19. Bold numbered samples are baseline condition.)

Condition	Charged	Burst Pressure (lb/in. <sup>2</sup> )	Uniform Strain	Failure Strain
BL-4	N	11,289	35.60	39.78
BL-1	Y	11,891	26.70	33.40
BL-2	Y	10,953	34.58	43.76
BL-3	Y	11,900	37.14	47.91
0.01 Notch 3	N	10,725	21.40	29.41
0.01 Notch 1	Y	11,608	25.43	34.35
0.01 Notch 2	Y	11,432	25.81	34.24
0.020 Notch 3	N	10,161	13.68	21.95
0.020 Notch 1	Y	10,356	14.26	22.37
0.020 Notch 2	Y	10,712	15.37	24.31
0.010 Notch LENS Repair 3	N	11,266	26.03	35.26
0.010 Notch LENS Repair 1	Y	11,944	27.42	33.92
0.010 Notch LENS Repair 2	Y	11,687	28.54	36.72
0.020 Notch LENS Repair 3	N	9,759	9.51	17.07
0.020 Notch LENS Repair 1	Y	10,594	13.70	20.20
0.020 Notch LENS Repair 2	Y	10,643	12.71	18.97
Vendor Certification	N	10,600		

tom corner easier to fully fill with LENS material and to reduce the stress riser. It is expected that this modification would make the failure much less likely to occur at the gouge location.

#### Metallographic Examination

Metallographic examination of selected samples was conducted. The samples were cut, polished, and electrolytically etched using a 10% oxalic acid solution. The samples were then examined on an inverted microscope and photographed at suitable magnifications to show the desired attributes.

The reclamation test base that was over-bored by 0.045 in. was selected for metallography after burst testing. A low-magnification view of the sample is shown in Fig. 23A. The fill stem foot is not parallel to the test base due to the burst testing. The edges of the welds may have been separated as well. Due to limited assets, metallographic examination was not conducted prior to testing. However, a typical reclamation weld of a baseline sample is shown in Fig. 23B. The welds generally exhibit 50 to 70% side bonding with a significant amount of extrusion on the top of the sample.

A comparison of the microstructure from a typical Type 304L SS reclamation weld reveals similarities and differences. The flow lines for both the stem foot as well as the base material are apparent. There are perceived differences in the relative amount and location of the material for the LENS-repaired sample compared to the standard base. The presence of flow lines in the LENS material is less apparent than for the fill stem bare stock. Note also the presence of fine porosity in the "corner" of the reclamation test base/LENS material. The LENS material seems to

have machined well as there is no indication of smearing on the chamfer at the bore centerline.

The sample bottles were also examined metallographically. A typical LENS repaired and machined sample is shown in Fig. 24. This sample exhibits some voids and porosity in the repair area. At least two different sample elevations were examined to verify the presence of these anomalies. The voids appear to be due to incomplete fusion of the laser-sintered powder to the bottle substrate. Higher magnification images clearly indicate that the bond is intermittent. The shape of the voids also indicate incomplete fusion as opposed to gas formation voids. It is surmised that a change in the bottle slot geometry to make the defect more weld repairable would have improved the nature of this repair. It is further expected that radiographic examination of the bottles prior to testing would have revealed these defects and perhaps have enabled a secondary fusion cycle to "heal" the voids. An optimized process certainly would have enabled higher-quality LENS repair techniques and material application to be implemented.

To better understand the nature of the fractures that were observed in the bottle burst tests, the fracture surfaces were examined using the scanning electron microscope. This examination revealed interesting results that support the findings of incomplete fusion that were observed in the optical microscopy. In Fig. 25, the edge of the machined notch can be seen adjacent to the powder fill that still shows sintered particles that retained their spherical geometry.

Ductile rupture was apparent for both the baseline and hydrogen-charged samples. There was no obvious change in the

dimple size between the hydrogen-charged samples and the baseline samples. In a well-bonded area of the LENS-repaired sample, there is evidence of ductile rupture with a very fine dimple size.

## Summary

Reclamation test bases that were overbored for both diameter and depth were successfully repaired using the LENS process. The material was machined and prepared in an acceptable manner for reclamation welding. Weld conditions identical to properly machined production-like test bases were successfully used for the LENS-repaired components. Baseline and hydrogen-charged reclamation test weld assemblies were burst tested with failures occurring in the fill stem wall at pressures consistent with expectations.

Gas sample bottles were machined to introduce a notch the length of the bottle that was 0.010 or 0.020 in. deep. Gas bottles with the notches were LENS repaired using a nonoptimized method. Gas sample bottles in the as-received, as-notched, and LENS-repaired conditions were hydrogen charged. Both hydrogen-charged and baseline gas sample bottles were hydroburst tested to failure. Hydrogen-charged samples exhibited slightly higher burst pressures and somewhat lower burst ductilities compared to baseline conditions. The strength of the LENS-repaired 0.010-in.-deep notch samples was slightly higher than the notched sample. With the exception of one sample, all of the LENS-repaired gas bottles failed in the LENS repair. The microstructure of the LENS-repaired material reveal incomplete fusion in a number of the overlay passes. The presence of unmelted particles at the fracture surface confirms inadequate heat.

It appears that LENS repair is highly suited for the repair of overbored reclamation-type materials.

Additional process development is required for weld repair of notched gas sample vessels. This development should include joint preparation in addition to thermal inputs and translation rates.

## References

1. Moskowitz, L. N., and Lindley, D. J. 1991. U.S. Patent 5019429, High density thermal spray coating and process. May 28, 1991.
2. Dalton, M., Transocean Offshore Deepwater Drilling Inc., May 2001. [www.nationalthermospray.com/RodRepair\\_Report2.htm](http://www.nationalthermospray.com/RodRepair_Report2.htm).
3. Nonaka, I., Ito, T., Ohsuki, S., and Takagi, Y. 2001. Performance of repair welds on aged 2.25 Cr-1 Mo boiler header welds. *International J. of Pres. Vessel and Piping* 78: 807-811.
4. Branza, T., Deschamps-Beaume, F., Velaya, V., and Lours, P. A microstructural and low-cycle fatigue investigation of weld-repaired heat-resistant cast steels. *J. Mat. Proc. Tech.* In press.
5. Welding for repair and surfacing, Key to steel. [www.key-to-steel.com/cz/de/Articles/Art129.htm](http://www.key-to-steel.com/cz/de/Articles/Art129.htm), Sept. 30, 2008.
6. Kim, J-D, Kim, C-J, and Chung, C-M. 2001. Repair welding of etched tubular components of nuclear power plant by Nd:YAG laser. *J. of Mat. Proc. Tech.* 114 (2001): 51-56.
7. Boy, J. H., Kumar, A., March, P., Willis, P., and Herman, H. 2008. Cavitation- and erosion-resistant thermal spray coatings. U.S. Army Corp of Engineers. [www.nationalthermospray.com/hydroele.htm](http://www.nationalthermospray.com/hydroele.htm), September 30.
8. Kanne Jr., W. R., Bruck, G. J., Madeyski, A., Lohmeier, D. A., Louthan Jr., M. R., Rankin, D. T., Shogan, R. P., Lessmann, G. G., and Franco-Ferreira, E. A. 1991. Weld repair of helium degraded reactor vessel material. *Fifth International Symposium on Environmental Degradation of Materials in Nuclear Power Systems - Water Reactors*, Monterey, Calif., August 25-29.
9. Yamada, H., Kawamura, H., Tsuchiya, K., Kalinin, G., Kohno, W., and Morishima, Y. 2002. Re-weldability tests of irradiated 316L(N) stainless steel using laser welding technique. *J. Nuclear Mat.* 307-311: 1584-1589.
10. Legg, K. 2000. HVOF in repair and overhaul — Higher reliability at lower cost?, Aviation Gas Turbine Engine O&R, Rowan Technology Group, Libertyville, Ill.
11. Tan, J. C., Looney, L., and Hashmi, M. S. J. 1999. Component repair using HVOF thermal spraying. *Journal of Materials Processing Technology* 92-93: 203-208.
12. Wu, X. W., Chandel, R. S., Seow, H. P., and Li, H. 2001. Wide gap brazing of stainless steel to nickel-based superalloy. *J. Mat. Proc. Tech.* 113: 215-221.
13. In-service weld metal deposition repair for pipelines, EWI tech brief, Sept. 30, 2008, and online, undated.
14. Qualification of LENS® for the repair and modification of NWC components project plan, version 2c, submitted to NNSA NA-123 — Office of Stockpile Technology, Readiness Campaign, Sept. 2004
15. Kanne, W. R. *50 Years of Excellence in Science and Engineering at the Savannah River Site*, p. 201.
16. Mao, X., Saito, M., and Takahashi, H. 1991. *Scripta Met* 25, pp. 2481-2485.
17. Foulds, J., Woytowicz, P., Parnell, T., and Jewett, C. 1995. *Journal of Testing and Evaluation* 23(1): 3-10.
18. Mao, X., and Takahashi, H. 1987. *Journal of Nuclear Materials* 150: 42-52.
19. Caskey, G. 1983. *Hydrogen Compatibility Handbook for Stainless Steels*, DP-1643, Savannah River Laboratory, Aiken, S.C., June.
20. Smugeresky, J., Keicher, D., and Grylls, R. 2003. Model Based Materials Processing for In-Space Fabrication, Presentation at In-Space Fabrication and Repair Research — An Industry-NASA-Academia Technical Forum, July.
21. Schlienger, E., Dimos, D., Griffith, M., Michael, J., Oliver, M., Romero, T., and Smugeresky, J. 1998. Near net shape production of metal components using LENS. *Proceedings, Pacific Rim International Conference on Advanced Materials and Processing*, Honolulu, Hawaii, July 1998.
22. Mazumder, J., Nagarathnam, K., Choi, J., Koch, J., and Hetzner, D. 1997. The direct metal deposition of H13 tool steel for 3-0 components. *Journal of Materials* 49(5): 55.
23. Griffith, M. L., Keicher, D. M., Atwood, C. L., Romero, J. A., Smugeresky, J. E., Harwell, L. D., and Greene, D. L. 1996. Free form fabrication of metallic components using laser engineered net shaping (LENS™). *Proceedings of the Solid Freeform Fabrication Symposium*, Aug. 12-14, Austin, Tex., p. 125.
24. Fessler, J. R., Merz, R., Nickel, A. H., Prim, F. B., and Weiss, L. E. 1996. Laser deposition of metals for shape deposition manufacturing. *Proceedings of the Solid Freeform Fabrication Symposium*, August 12-14, Austin, Tex., p. 117.
25. Klocke, F., Wirtz, H., and Meiners, W. 1996. Direct manufacturing of metal prototypes and prototype tools. *Proceedings of the Solid Freeform Fabrication Symposium*, Aug. 12-14, Austin, Tex., p.141.
26. Morgan, M. J. 2008. Hydrogen effects on the fracture toughness properties of forged stainless steels. *Proceedings of PVP2008 2008 ASME Pressure Vessels and Piping Division Conference*, July 27-31, Chicago, Ill.
27. Morgan, M. J., and Chapman, G. K. 2009. Hydrogen effects on fracture toughness of Type 316L stainless steel from 175 K to 425 K. *Proceedings of PVP2009 ASME Pressure Vessels and Piping Division Conference*, July 27-30, Prague, Czech Republic.
28. Morgan, M. J., Hall, M., Lam, P-S, and Thompson, W. D. 2008. Hydrogen effects on the burst properties of Type 304L stainless steel flawed vessels. *Proceedings of PVP2008, 2008 ASME Pressure Vessels and Piping Division Conference*, July 27-31, Chicago, Ill.
29. Krishna, B., Bose, V., and Bandyopadhyay, A. 2009. A fabrication of porous NiTi shape memory alloy structures using laser engineered net shaping. *Journal of Biomedical Materials Research Part B* 89(2): 481-490.
30. ASME SA-312/SA-312M, *Specification for Seamless and Welded Austenitic Stainless Steel Pipes*. 2009. ASME, New York, N.Y.
31. Hearn, E. J. 1997. *Mechanics of Materials, Volume 1 — An Introduction to the Mechanics of Elastic and Plastic Deformation of Solids and Structural Materials* (3rd Edition). Elsevier., p 198. Online version available at: [www.knovel.com/webportal/browse/display?\\_EXT\\_KNOVEL\\_DISPLAY\\_bookid=432&VerticalID=0](http://www.knovel.com/webportal/browse/display?_EXT_KNOVEL_DISPLAY_bookid=432&VerticalID=0).